Proceedings World Geothermal Congress 2010
Bali, Indonesia, 25-29 April 2010

A Resource Conceptual Model for the Ngatamariki Geothermal Field Based on Recent Exploration Well Drilling and 3D MT Resistivity Imaging

Catherine Boseley[1], William Cumming[2], Luis Urzúa-Monsalve[3], Tom Powell[1] and Malcolm Grant[4]

[1]Mighty River Power, P.O. Box 445, Hamilton, New Zealand

[2]Cumming Geoscience, 4728 Shade Tree Lane, Santa Rosa CA 95405, USA

[3]Hot Rock Ltd., Level 9, BNZ tower, 125 Queen Street, Auckland 1000, New Zealand

[4]MAGAK, 208D Runciman Rd, RD2, Pukekohe 2677, New Zealand

Catherine.Boseley@MightyRiver.co.nz

Keywords: Ngatamariki, MT, conceptual model, alteration, hydrology, geothermal exploration

ABSTRACT

Three successful exploration step-out wells drilled by Rotokawa Joint Venture (RJV) in 2008-2009 at the Ngatamariki Geothermal Field helped demonstrate sufficient resource to support regulatory applications for over 100 MW of generation. This field was discovered in 1984 when four wells were drilled and two wells, about 1 km apart, encountered a permeable 280ºC resource. However, economic and access complications halted further drilling. After initial access was obtained in 2004, RJV conducted MT surveys and completed risk assessments based on a range of conceptual models that supported relatively aggressive well targeting 1.6 to 3 km south of the earlier wells.

The resource conceptual models were constrained by integrated interpretations that focused on well results, geochemistry and MT resistivity. The geochemistry from hot springs and well fluids indicated that the hot springs were supplied through a 160ºC intermediate aquifer, not directly from the reservoir. The natural state temperature pattern, flow performance, alteration, and geology data from the wells established the elements of the model that were extrapolated beyond the drilled area using the MT imaging of aquicludes that contained low resistivity smectite clay associated with low permeability.

The base-case resource model used in 2008 to target the wells included five main elements. Two smectite-rich aquicludes separated three permeable zones; a 15ºC meteoric aquifer, a 160ºC intermediate aquifer near the initial wells, and a deep 260 to 300ºC geothermal reservoir that extended 3 km south of the initial wells. The basic conceptual scheme was confirmed as new well test data became available and as the resistivity imaging was updated based on revised TDEM corrections to 1D MT inversions and new 3D MT inversions of larger data sets. New details included a reinterpreted deep fractured upflow 1 km north of its initial location and a thin 150ºC permeable zone interpreted within the clay cap. The resource conceptual model presented here was the basis for further reservoir analyses and the numerical simulation of development options such as injection targeting to optimize long term performance.

1. INTRODUCTION

More than 21 high enthalpy geothermal reservoirs and prospects have been identified within the Taupo Volcanic Zone (TVZ), New Zealand (Figure 1). Development has been prohibited or limited at seven prospects. As changes in power price and access have made new investment attractive, geothermal developers have drilled new wells at the five developed reservoirs to increase generation. Exploration surveys and access negotiations at prospects in the TVZ led to the identification of Ngatamariki as an attractive candidate resource to support a new power plant.

The Ngatamariki geothermal field is located in the central part of the TVZ about 25 km northeast of Lake Taupo (Figure 1). Schlumberger profiling detected a 7 to 12 km^2 shallow low resistivity area near hot springs, leading to the drilling of four deep wells in 1984 (Figure 2). Two wells, NM2 and NM3 discovered a high permeability resource with temperature over 280°C. Despite these promising results, the initial drilling was not followed up due to low power prices, testing limitations and access issues. After initial access was secured in 2004, Rotokawa Joint Venture (RJV), a joint venture between Tauhara North #2 Trust and Mighty River Power, acquired over 86 MT and TDEM stations to improve targeting of new wells and assess the geothermal resource capacity at Ngatamariki.

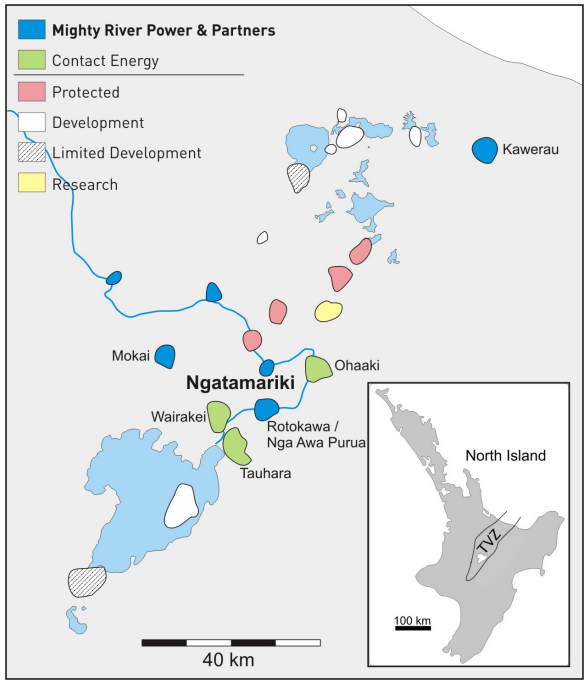

Figure 1: Location map. Ngatamariki is located in the Taupo Volcanic Zone near five developed geothermal fields.

The most prominent feature in the MT resistivity pattern at Ngatamariki is the low resistivity, low permeability smectite clay cap that overlies the higher resistivity, higher temperature, and higher permeability productive reservoir (Figure 3). This close correlation of low resistivity with high smectite clay and low permeability is consistent with the pattern detected at other geothermal fields in New Zealand and with most published case histories at geothermal fields worldwide (Ussher, 2000). Zones with significant smectite and mixed layer smectite-illite clay act as barriers to fluid flow. Even where penetrated by fractures, such clays inhibit the creation of permeable open space (Davatzes and Hickman, 2009). Some rocks that are less likely to have much smectite clay alteration, like rhyolite lavas, can form permeable fluid conduits through a clay cap. An alternating sequence of layers, some with abundant smectite and others with little, can produce several aquifers and aquicludes over a geothermal reservoir (Bowyer and Holt, 2010).

Smectite and smectite-illite clays are the predominant hydrothermal alteration products formed in the weakly acidic waters found over and adjacent to geothermal reservoirs from 70 to 200ºC (Simmons and Browne, 1998). However, in New Zealand, other sources of smectite are commonly found near geothermal reservoirs. Shallow lake beds associated with the extensional subsidence along the central axis of the TVZ, generically called the Huka Falls formation, are low in resistivity where they consist of mudstones with high smectite content. Devitrification of ignimbrites can produce smectite and zeolite alteration (Bibby et al, 1999) and paleosedimentary basins often include shale. Ngatamariki well cuttings descriptions and MeB and XRD clay analysis (Gunderson et al., 2000) confirm the presence of smectite in the Huka Falls formation and in a deeper hydrothermal smectite cap. The flat-lying resistivity pattern and slightly higher resistivity typical of the non-hydrothermal sources of smectite are used as a diagnostic indication of conceptual model uncertainty at Ngatamariki (Urzúa-Monsalve, 2008).

Following an outline of how bore hole, resistivity, geology and hot spring data were used to build conceptual models and target wells NM5A, NM6 and NM7, a revised conceptual model is presented based on the results of all of the wells. The revised model is surprising similar to the original of Urzúa-Monsalve (2008) given the large step-out distances of 1.6 and 3 km from the original wells. The hydrologic model elements are basically unchanged, although the location of the upflow shifted north and a thin permeable zone within the clay cap was added. Because drilling has proven the resource along a north-south axis, the most confident areas are now more elongated in that direction in Figure 3 than they were in Urzúa-Monsalve (2008). Resistivity cross-sections and maps from a newer 3D MT resistivity inversion that includes all available MT data illustrate the revised rationale for the Ngatamariki resource outline at two confidence levels shown in Figure 2.

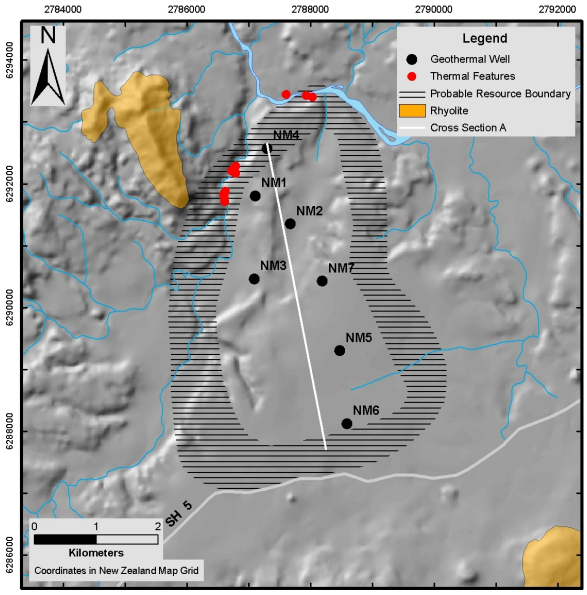

Figure 2: Map of the Ngatamariki geothermal field showing the wells, hot springs, surface exposure of rhyolite lavas that act as cold water collectors, the resource boundary defined by two confidence levels, and the profile of the conceptual cross-section A.

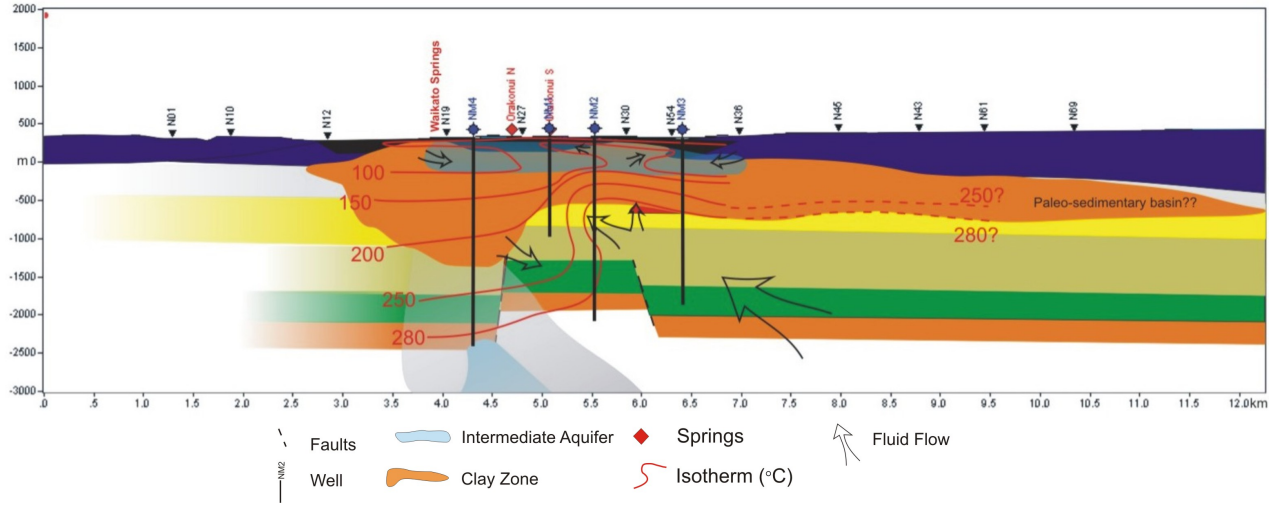

Figure 3: Extended cross-section A illustrates the RJV resource conceptual model used to target wells NM5A, NM6 and NM7 at Ngatamariki Field based on 1D MT resistivity cross-sections, well natural state temperature, lithology and alteration and hot spring geochemistry. In this conceptual model illustration, the deep upflow is interpreted south of NM3 and rises up to the north on the left (after Urzúa-Monsalve, 2008).

2. EXPLORATION STEP-OUT TARGETING

RJV 's initial assessment of Ngatamariki detailed in Urzúa-Monsalve (2008) used an interpretation approach that emphasized resource conceptual models consistent with the MT resistivity images in map and section view as well as with the geochemistry, alteration and interpreted temperature data from the wells and hot springs (Cumming, 2009). Exploration targeting at Ngatamariki in the 1980s had relied, in part, on analogies to particular Schlumberger profiling resistivity contours that loosely correlated with resource boundaries at other fields, an approach that Ussher (2007) showed could be misleading. When targeting the Ngatamariki wells in 2008 and 2009, all of the data sets were evaluated within the context of the resource conceptual model and uncertainty was assessed not by considering a range of particular resistivity contours but by considering confidence levels for drilling success based on what range of conceptual model parameters was consistent with the available data.

Urzúa-Monsalve (2008) integrated resistivity cross-section images derived from stitched 1D MT inversions with the alteration and geochemistry data from wells and springs to produce a resource conceptual model with two impermeable and three permeable layers (Figure 3). A surface meteoric aquifer was separated by the Huka Falls formation from a 160 to 180ºC intermediate aquifer that locally leaked to the surface and mixed with meteoric water to form the hot springs. This aquifer was weakly connected to the 270 to 300ºC reservoir through a deeper leak in the hydrothermal clay cap. To characterize the uncertainty in targeting the deep reservoir, areas and confidence levels consistent with a lognormal probability distribution were based on the interpreted natural state temperature pattern, extrapolated using the 1D MT resistivity images. Multiple models allowed for different geological assumptions regarding the hydrothermal origin of the clays associated with the deeper low resistivity zone. The basin clay label in Figure 3 illustrated one such option. A 3D MT inversion was also used to assess uncertainty in the resistivity images but the interpretation focused on the 1D MT inversion because, at the time, it better resolved shallow resistivity and included data from follow-up surveys and from the adjacent Rotokawa field.

Based on these results a follow-up drilling program was designed to efficiently prove adequate resource capacity for a development. Well NM5A was proposed as a significant step-out 1.6 km southeast of NM3 that was given >50% chance of success because it was near a local high in the base of the clay cap (Urzúa-Monsalve, 2008), characteristic of a local permeable apex in a reservoir (Cumming et al., 2000). A further step-out to NM6, 3 km south of NM3, was based on weighting several alternative models, including proximity to a local inflection in the base of the clay cap, and the possibility that the low resistivity pattern might be associated with deep sediments noted at the right side of Figure 3. Other possibilities included altered ignimbrites, marginal clays and the possibility that local resistivity variations were due to unreliable MT data related to noise, static shift or 3D distortion. The overall north-south trend and a transition to slightly higher resistivity to the south in both 1D and 3D inversions led to this well being assigned a <50% chance of success, a relatively bold step-out that was given high value because of its potential implications for resource capacity. NM7 was targeted about 1 km east of NM3 close to the interpreted upflow. With the success of all of these wells, the focus has shifted to issues required to get regulatory approvals to develop the resource.

3. CONCEPTUAL MODEL ELEMENTS

The revised conceptual model is illustrated in three cross-sections. Figure 4 shows the natural state isotherms, well entry zones within the reservoir, primary rock types and the zone of smectite clay alteration. Figure 5 shows the isotherms overlaid on the interpreted hydrological zonation within the reservoir. The 3D MT resistivity image along this profile in Figure 6 illustrates how the interpretation of the probable resource area is extended beyond the area with well control. The wells and isotherms are included on each figure to provide a common conceptual reference.

The isotherm pattern shown in Figures 4 to 6 is based on well measurements that are probably representative but perhaps still slightly disturbed by drilling or testing. The temperature patterns mark both the lateral extent of the resource and the vertical zonation into separate aquifers. A conductive thermal gradient indicates a low permeability aquiclude. If the gradient is high, crowding isotherms, the aquiclude is bordered by contrasting hot and cold aquifers (Cumming, 2009). Isothermal sections are usually permeable aquifers. Although consistent contour interval spacing is important to interpreting temperature gradients from isotherms, the contour interval in Figures 4 to 6 has one irregular interval between 250 to 275ºC in order to illustrate the reservoir top effectively without obscuring the figure with contours. The conceptual model elements indicated by the temperature pattern are described from the deepest isotherms to the shallowest.

3.1 Permeable Reservoir and Deep Upflow

The relationship of the temperature gradient to permeability and the smectite-illite transition is most clearly illustrated at the top of the reservoir between wells NM2 and NM6. An increase in the vertical thermal gradient at the top of the isothermal reservoir corresponds to the base of the smectite zone, shown as a hachured pattern. As illustrated in Figure 5, the top of the isothermal reservoir is near 275ºC at NM2, NM3 and NM7 and decreases laterally away from these wells that are closest to the upflow zone.

The base of the smectite clay cap detected by the MT resistivity shown in Figure 6 is conformable to the top of the underlying reservoir but the base of the lowest resistivity zone from 1 to 7 ohm-m (red to yellow) roughly follows the 150ºC contour, not the 275ºC reservoir top. This is consistent with the MeB measurements of clay content in the wells. Smectite clay is more abundant in the Wairakei Ignimbrite than in the Tahorakuri andesite lavas below it. A pattern where the base of the lowest resistivity clay zone is conformable to but shallower than the top of the permeable reservoir is commonly encountered in geothermal case histories (Cumming et al., 2000) and can be incorporated into the resource conceptual model by using the resistivity patterns at the existing wells as analogies to predict the likely isotherm pattern at undrilled field margins.

The 1D MT inversions shown in Figure 3 give the impression of a deeper extent of clay alteration, perhaps corresponding to the smectite alteration in the Tahorakuri formation. A better correlation of 1D MT inversions with alteration is sometimes observed where the MT stations are not close to lateral boundaries that would cause 3D distortion and where the 3D MT inversion overly smoothes the vertical variations in resistivity to avoid large inversion artifacts (Cumming and Mackie, 2007). The interpretation addresses this ambiguity by considering both 1D and 3D inversion images in the assessment of conceptual model uncertainty.

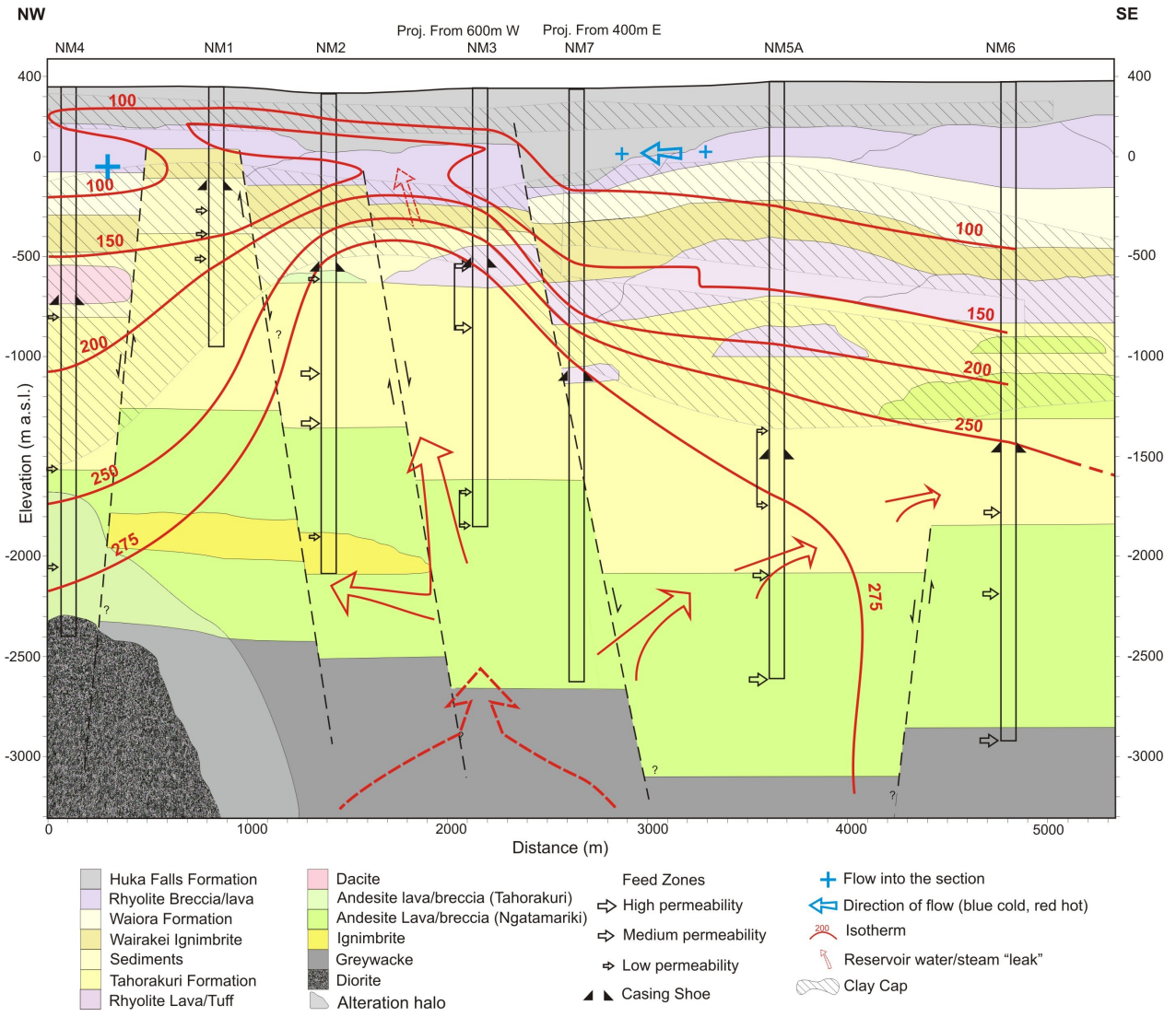

Figure 4: Conceptual model of the Ngatamariki Geothermal Field illustrated with isotherms, production entries, geology, smectite clay alteration and interpreted flow patterns based on all seven wells.

The relatively low temperatures and conductive gradient below -1000 masl in NM4 at the north end of the profile are shown in Figure 3 as potentially marking a north boundary for the resource and possibly acting as a permeability barrier on the north side of the field. The major fault offset shown in the cross-section is based on well results but it is not mapped at the surface (Wood, 1986). As shown in Figure 4, if the reservoir extends this far north, it will be deep, as reflected in the resource outline in the map in Figure 2. The quartz diorite intrusion penetrated by NM4 has a high temperature magmatic alteration halo of quartz, illite/muscovite, and pyrite that should be high resistivity as shown in Figure 6. The much deeper low resistivity zone in Figure 3 correlates better with the temperature pattern; however, this is probably coincidental because 3D MT distortion at shallow depths related to an adjacent rhyolite lava makes the 1D MT inversions unreliable.

The reversal in temperature at the bottom of well NM1 and slight reversals in NM2 and NM3 between -1600 and -2000 masl are interpreted in Figure 3, prior to drilling NM5A, as indicating that the deep upflow is located more than 1 km south of NM3. This was also consistent with a local resistivity high in the base of the clay cap in Figure 3. However, the slightly cooler temperatures measured in NM5A point to an upflow farther north, generally centered between NM3 and NM7 as shown in Figure 4. The 3D MT inversion in Figure 6 suggests that the apparent doming may have just been just less intense alteration, whereas doming over an upflow is usually associated with thinner but more intense alteration.

The entries in NM6, its temperature over 250ºC, and the nearly isothermal gradient imply that the reservoir extends to this area at least 3 km to the south of NM3, consistent with the pattern predicted by Urzúa-Monsalve (2008) in Figure 3. However, the 25ºC lateral reservoir temperature decrease between NM5A and NM6 implies that NM6 may be near the edge of the reservoir. Although the predicted reservoir extent and general shape have been confirmed, because the reservoir is cooler as well as deeper to the south, the southern area is more likely to be an attractive target for injection than for production.

The geochemistry of fluids produced from the wells is typical for a neutral chloride geothermal reservoir, with Na-K geothermometry of 300ºC, a temperature not yet measured in a well.

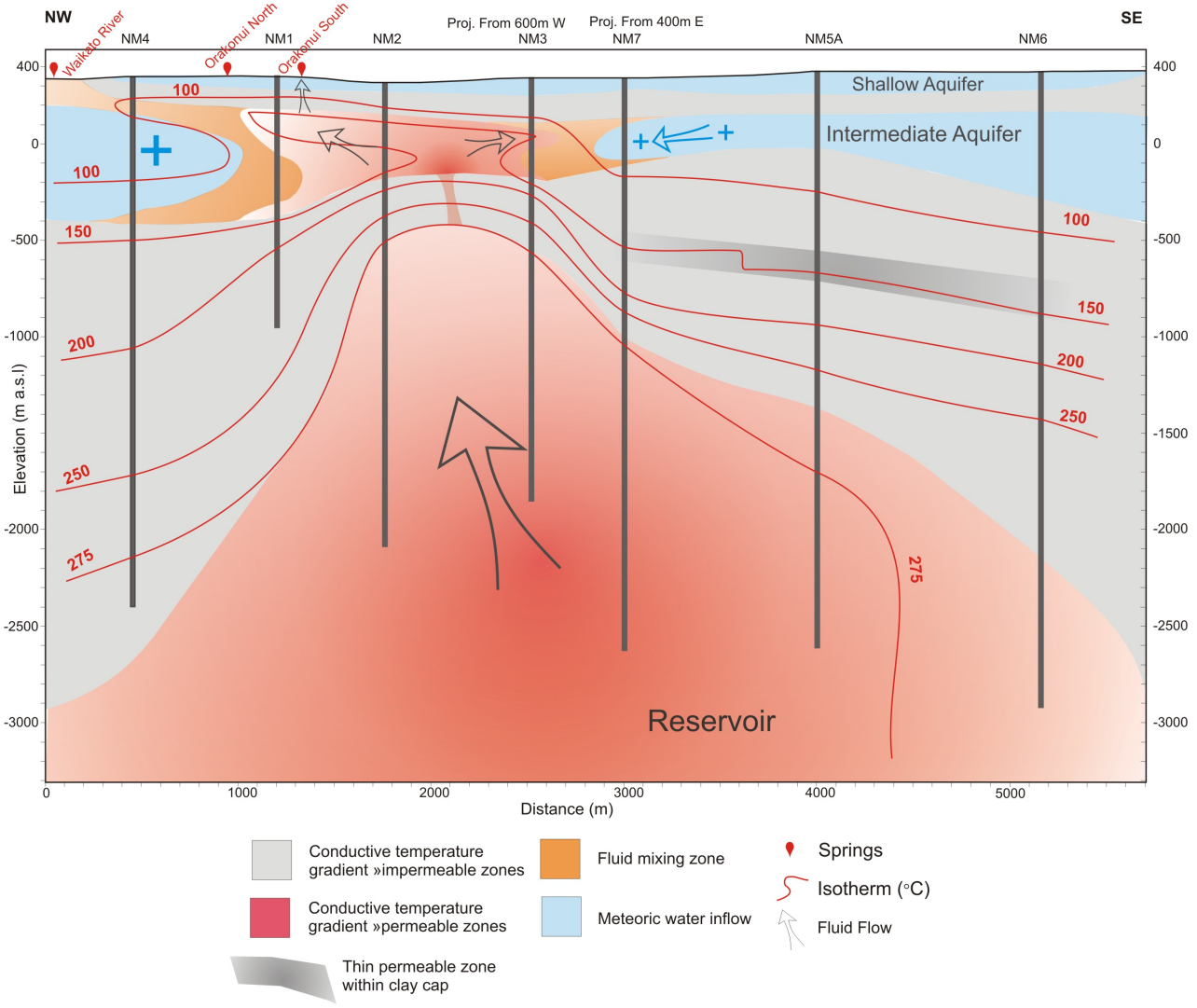

Figure 5: Hydrological zonation of the of the Ngatamariki geothermal reservoir with isotherms, hot and cold aquifers, wells and hot springs.

3.2 Thin 150º Permeable Zone at -600 masl to South

A thin permeable zone at ~150ºC is illustrated in Figures 4 and 5 at about -600 masl south of NM7. The vertical kink in the 150ºC contour between NM7 and NM5A reflects the adjacent isothermal sections in NM6 and NM5A. This zone appears to be isolated within the clay cap and so may mark a zone of cross-flow out of the section. This zone partly follows dacite/rhyolite lavas between the Wairakei Ignimbrite and the Tahorakuri formation. The permeability is consistent with low MeB measurements for smectite clay, illustrated by the gap in hachured pattern. Although it may not impact reservoir performance, it may present drilling challenges, as suggested by high mud losses in NM6.

3.3 Hydrothermal Clay Cap

Besides the critical role the base of the hydrothermal smectite clay cap plays in defining the top of the geothermal reservoir, it also performs an important role as the base of any overlying aquifers, which the clay cap isolates from the reservoir. Based on MeB measurements on cuttings and the pattern of resistivity in Figure 6, the Ngatamariki clay cap is less than 400 m thick at wells NM2 and NM3 and rapidly thickens to over 1000 m away from this zone. The thinned clay cap likely reflects the proximity of the deep fractured upflow centered just to the south, the common structures that promoted through-going permeable pathways between the deep upflow and this shallow zone, and the tendency of smectite to be converted to illite at the higher temperatures that would prevail in these circumstances. Although it is probably too small to be explicitly imaged using MT, the higher temperatures above the clay cap in NM1, NM2 and NM3 imply that a permeable pathway must connect the deep reservoir through the clay cap to the overlying aquifer. This is included in Figure 5 as a narrow conduit off the line of section so the isotherms are not disturbed.

3.4 Intermediate Cold and Hot Aquifers

An intermediate aquifer between the reservoir and the cold surface aquifers is found in all of the wells near sea level. It is associated with rhyolite lavas and breccias and is commonly very permeable based on total drilling loses. In the wells that are farthest from the leak through the clay cap, NM4, NM5A, NM6 and NM7, this aquifer is relatively cold (blue in Figure 5) due to cross-flow in the regional aquifer and locally induced downward flow from rhyolite surface exposures (Figure 2).

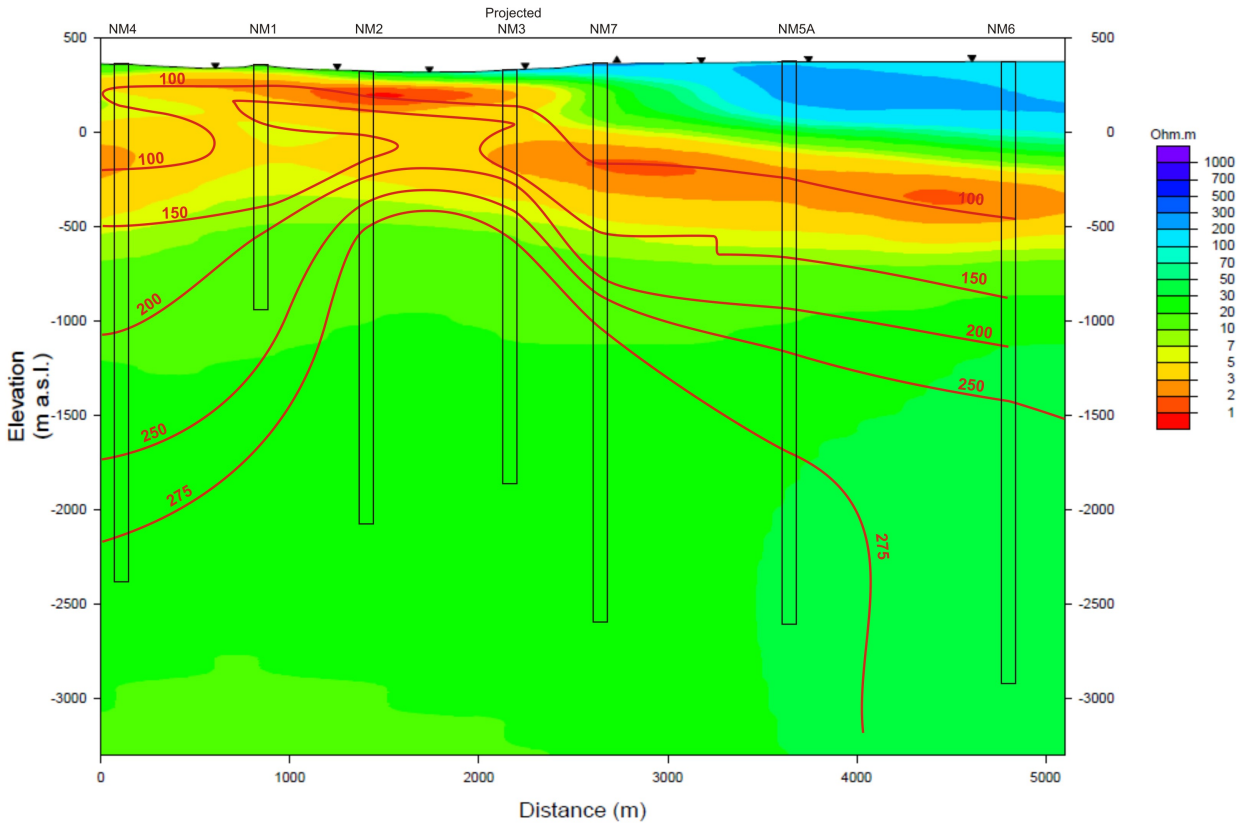

Figure 6: Cross-section showing 3D MT resistivity at the Ngatamariki geothermal reservoir with MT stations, isotherms and wells.

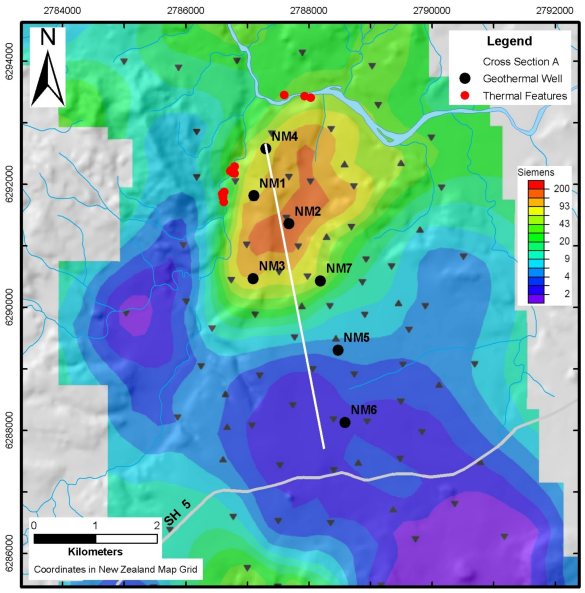

Figure 7: Conductance from surface to sea level (0 masl) based on 3D MT inversions. This is interpreted as being analogous to the total smectite clay content in this interval, with red-yellow being a high clay impermeable zone and blue a low clay, potentially permeable zone.

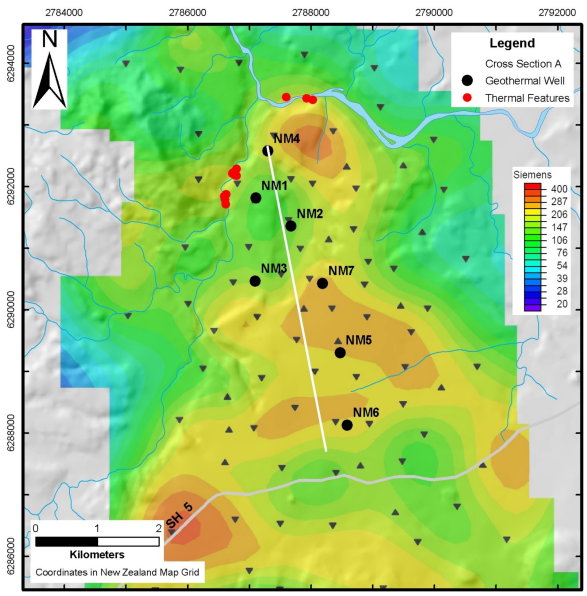

Figure 8: Conductance from sea level to -1000 masl based on 3D MT inversions. This is interpreted as being analogous to the total smectite clay content in this interval, with red-yellow being a high clay impermeable zone and green-blue a low clay, potentially permeable zone.

The pattern of isotherms between sea level and 200 masl in NM1, NM2 and NM3 in Figures 4 and 5 indicate that the intermediate zone is permeable and locally heated from below by a leak in the underlying hydrothermal clay cap.

These hot fluids leak up from this zone and reach the surface at the hot springs Orakonui north, Orakonui south and the Waikato River as suggested by the outflow interpreted from the 100 and 150ºC isotherms.

The intermediate aquifer has chloride-bicarbonate water chemistry, consistent with mixing of shallow ground water and deeper geothermal fluids. No hot spring has a chloride concentration over 1000 ppm that might hint of a direct connection to the high temperature deep reservoir. The hot spring Na-K-Mg geothermometry of 140 to 170ºC is consistent with hot springs being a mixture of water from the surface meteoric aquifer with water from the intermediate aquifer shaded in red near sea level between NM1 and NM5A in Figure 5 (Urzúa-Monsalve, 2008). Moreover, the consistency of the geothermometry suggests that the intermediate aquifer fluids themselves reach a local equilibrium and are not closely connected to the deep reservoir with its 300ºC geothermometry. This is supported by the high measured temperature gradient between the intermediate aquifer and the reservoir. For these reasons, the leak from the reservoir to the intermediate aquifer is shown as a narrow neck between the two zones.

3.5 Huka Falls Claystones

The Huka Falls claystones cap the intermediate aquifer and separate it from the overlying cold meteoric aquifer. Such claystones are typically very low in resistivity over geothermal fields. The cross-section in Figure 6 shows that leakage from the intermediate aquifer finds its way to the surface at the northern edge of the part of this zone with the highest concentration of smectite clay. The map of conductance from surface to sea level in Figure 7 provides an indication of the Huka Falls clay over that range in elevation that has been affected by interaction with the underlying reservoir. The hot springs appear around the edges of the zone with highest smectite content. Therefore, these claystones cap the intermediate aquifer, and only indirectly indicate the geometry of the underlying reservoir.

3.6 Surface Aquifer

A 15 to 20ºC, surface aquifer that extends to 50 m depth is shown in blue in Figure 5 over the entire area, except where the intermediate aquifer leaks to the surface at the north end of the cross-section. It is isolated from deeper aquifers by the impermeable Huka Falls claystones.

The exposed rhyolite lavas shown in Figure 2 likely induce a local pressure regime in shallow aquifers that is added to the regional piezometric gradient that controls cold water that enters the perimeter of the resource area. The necks of these rhyolite domes are likely to function as conduits to the underlying rhyolites of the intermediate aquifer. Therefore, the temperature reversal near sea level in NM4 and NM1 may reflect influx of water from the northern dome in Figure 2. This fits the resistivity pattern imaged by the MT at shallow depths, in Figure 7. Therefore, the dark blue in Figure 7 probably indicates the low clay content of shallow, permeable, cold aquifers, mainly consisting of rhyolite flows and breccias.

5. RESOURCE PERIMETERS FROM MT

To extrapolate the resource conceptual model beyond the wells in order to target new wells and assess resource capacity, the MT pattern where there is no well control is compared to the resistivity pattern at the wells. The interpretation focuses on the deeper low to high resistivity transition corresponding to the hydrothermal alteration transition from smectite to illite, not the shallower pattern related to the Huka Falls claystones. MT cross-sections based on both 1D and 3D inversions were compared to characterize the uncertainty in the boundary, although in some cases only one inversion method was emphasized; for example, at MT stations that showed indications of significant 3D distortion, the 3D inversion would be emphasized, like near well NM4. Two versions of the 1D inversion were also considered. One version omitted TDEM corrections at all stations and the other omitted TDEM corrections only at stations with a thick section of resistive rocks at the surface that would likely distort the TDEM results (Urzúa-Monsalve, 2008; Cumming and Mackie, 2010). These sources of local uncertainty in the resistivity pattern and in its conceptual meaning were finally reviewed in the context of case histories of resistivity in other TVZ geothermal fields.

To estimate a resource boundary, a conceptual outline was defined based on a consistent pattern shared among about twenty 3D and many 1D MT cross-sections that crossed the resource area, mainly along east-west profiles. The conceptual relationship of the MT images relative to the existing wells was extrapolated to other areas by analogy. A level of confidence in the conceptual analogy and the MT data was subjectively associated with a cumulative probability that fit a lognormal area distribution. The validity of this estimate was tested using comparisons to conceptual models for other geothermal reservoirs and to other resource assessment methods, including reservoir engineering analyses based only on well data and analogies to other fields.

Four boundaries were defined based on the following criteria.

1) A deep upflow boundary was based on a subtle high in the base of the clay cap imaged in the 3D MT inversion and lower than usual resistivity on two MT stations between wells NM3 and NM7.

2) A boundary associated with over 80% confidence in targeting successful wells was based on an inflection to a higher elevation in the base of the low resistivity cap, as illustrated in Figure 6 about half way between NM5A and NM6. This outlines NM2, NM3, NM5A and NM7 with a 200 to 400 m margin.

3) An outline representing an area where expectations for a successful well exceed 50%, sometimes called a P50 size, was based on an analogy to the low resistivity slab of alteration like that in Figure 6 at sea level to -1000 masl from NM7 to NM6, with a rough map distribution for it illustrated by Figure 8. Although there are many counter-examples where such a feature overlies hot but low permeability rocks, the experience at NM6 compensates for those negative case histories with its success and proximity. This corresponds to the inner boundary of the hachured pattern shown in Figure 2, enclosing about 10 km^2.

4) An outer fringe where the resistivity in the smectite cap begins to rise, indicating less hydrothermal alteration and/or the flat geometry, looks like sediments. The likelihood of a successful well at this perimeter was assumed to be below 20%, enclosing about 21 km^2. To the south and west of NM5A, the low resistivity zone becomes flat, losing the doming appearance. This is suggestive of an impermeable ignimbrite or sediment. Therefore, there was significant risk in the interpretation of this area as permeable resource at over 275 ºC. The main criterion used to define the absence of the reservoir was the absence of alteration.

9. CONCLUSIONS

The elements of a robust resource conceptual model for the Ngatamariki Geothermal Field were initially developed using data from four wells drilled in the 1980s, hot spring

geochemistry and 1D resistivity images from a new MT survey. Based on this conceptual model, two step-out wells, NM5A and NM6, were successfully targeted on an extension of the resource 3 km to the south, while well NM7 was targeted on the deep upflow. The basic elements of the conceptual model were confirmed by the step-out wells. Although temperatures have not fully stabilized, preliminary tests indicate that well NM7 may have the highest temperature and is likely to be the most productive of the wells to date. Further analyses based on the resource conceptual model are directed at planning for a 100 MW power plant development.

The pattern of low resistivity from 1D and 3D MT inversions generally matches the distribution of smectite clay alteration associated with low permeability aquicludes. Two distinct aquicludes are detected, a deeper one corresponds to hydrothermal smectite clay alteration that caps the >270ºC reservoir. The shallower smectite zone caps a ~160 to 180ºC intermediate reservoir hosted in rhyolite lavas and separates it from an overlying cold meteoric aquifer. All of the well and hot spring data together with the updated 1D and 3D MT resistivity imaging were important in confirming the essential elements of the initial conceptual model and proposing a revised strategy for further development. This conceptual model, including the shallow and intermediate aquifers, has been integrated in a reservoir simulation model to assess strategies for developing 100 MW of generation at Ngatamariki.

10. REFERENCES

Boyer, D., and Holt, R., 2010. Case Study: Development of a Numerical Model by a Multi-Disciplinary Approach, Rotokawa Geothermal Field, New Zealand. Proceedings World Geothermal Congress 2010.

Browne, P.R.L.: 1989. Contrasting Alteration Styles of Andesitic and Rhyolitic Rocks in Geothermal Fields of the Taupo Volcanic Zone, New Zealand. Proc. 11th New Zealand Geothermal Workshop, 1989. University of Auckland: 111-116.

Browne, P.R.L., Graham, I.J., Parker, R.J., Wood, C.P., 1992. Subsurface Andesite Lavas and Plutonic Rocks in the Rotokawa and Ngatamariki Geothermal Systems, Taupo Volcanic Zone, New Zealand. Journal of Volcanology and Geothermal Research, 51(3): 199-215.

Cumming, W., Nordquist, G., and Astra, D., 2000, Geophysical Exploration for Geothermal Resources, an Application for Combined MT-TDEM. 70th Ann. Internat. Mtg., Soc. Expl. Geophys., Expanded Abstracts.

Cumming, W., 2009. Geothermal Resource Conceptual Models using Surface Exploration Data. *Proceedings*, 34th Workshop on Geothermal Reservoir Engineering, Stanford University, Stanford, CA.

Cumming, W., 2010. Geothermal Resistivity Imaging of Geothermal Resources using 1D, 2D and 3D MT Inversion With and without TDEM Static Shift Correction Illustrated by a Glass Mountain Case History. Proceedings World Geothermal Congress 2010.

Davatzes, N. and Hickman, S., 2009. Fractures, Stress and Fuid Flow Prior to Stimulation of Well 27-15, Desert Peak, Nevada, EGS Project. *Proceedings*, 34th Workshop on Geothermal Reservoir Engineering, Stanford University, Stanford, CA.

Gunderson, R., Cumming W., Astra D., and Harvey, C., 2000. Analysis of Smectite Clays in Geothermal Drill Cuttings by the Methylene Blue Method.: for Well Site Geothermometry and Resistive Sounding Correlation. Proceedings World Geothermal Congress 2000. Kyushu – Tohoku, Japan, May 28 – June 10, 2000.

Spinks, K., Powell, T., Siega, C., and Bardsley, C., 2010. Mighty River Power's Resource and Development Strategy at Kawerau Geothermal Field, New Zealand. Proceedings World Geothermal Congress 2010.

Urzúa-Monsalve, L.A., 2008. Integration of a Preliminary One-Dimensional MT Analysis with Geology and Geochemistry in a Conceptual Model of the Ngatamariki Geothermal Field. M.S. Thesis. University of Auckland. 128 p.

Ussher, G., 2007. Resistivity Case Histories. Geothermal Resources Council Annual Meeting 2007. Geophysics Short Course PowerPoint.

Ussher, G., Harvey, C., Johnstone, R., Anderson, E., 2000. Understanding the Resistivities Observed in Geothermal Systems. Proceedings World Geothermal Congress 2000. 1915-1920.

Wood, C.P., 1986. Stratigraphy and Petrology of NM4 Ngatamariki Geothermal Field. DSIR report.